Published online 29 March 2008

Nucleic Acids Research, 2008, Vol. 36, No. 8 ***2787–2798***
doi:10.1093/nar/gkn144

A BBP–Mud2p heterodimer mediates branchpoint recognition and influences splicing substrate abundance in budding yeast

Qiang Wang[1], Li Zhang[1], Bert Lynn[2] and Brian C. Rymond[1,*]

[1]Department of Biology and [2]Department of Chemistry, University of Kentucky, Lexington, KY 40506-0225, USA

Received November 30, 2007; Revised February 27, 2008; Accepted March 14, 2008

ABSTRACT

The 3′ end of mammalian introns is marked by the branchpoint binding protein, SF1, and the U2AF65-U2AF35 heterodimer bound at an adjacent sequence. Baker's yeast has equivalent proteins, branchpoint binding protein (BBP) (SF1) and Mud2p (U2AF65), but lacks an obvious U2AF35 homolog, leaving open the question of whether another protein substitutes during spliceosome assembly. Gel filtration, affinity selection and mass spectrometry were used to show that rather than a U2AF65/U2AF35-like heterodimer, Mud2p forms a complex with BBP without a third (U2AF35-like) factor. Using mutants of *MUD2* and *BBP*, we show that the BBP–Mud2p complex bridges partner-specific Prp39p, Mer1p, Clf1p and Smy2p two-hybrid interactions. In addition to inhibiting Mud2p association, the *bbpΔ56* mutation impairs splicing, enhances pre-mRNA release from the nucleus, and similar to a *mud2::KAN* knockout, suppresses a lethal *sub2::KAN* mutation. Unexpectedly, rather than exacerbating *bbpΔ56*, the *mud2::KAN* mutation partially suppresses a pre-mRNA accumulation defect observed with *bbpΔ56*. We propose that a BBP–Mud2p heterodimer binds as a unit to the branchpoint *in vivo* and serves as a target for the Sub2p-DExD/H-box ATPase and for other splicing factors during spliceosome assembly. In addition, our results suggest the possibility that the Mud2p may enhance the turnover of pre-mRNA with impaired BBP-branchpoint association.

INTRODUCTION

Pre-mRNA splice site consensus sequences are sampled multiple times during spliceosome assembly (1). For example, early in assembly the yeast 5′ splice site is bound by the U1 snRNP particle through protein and snRNA-based contacts. U1 snRNP also interacts with the branchpoint region through association with the branchpoint binding protein (BBP), a homolog of the mammalian SF1 protein (2,3). Subsequent recruitment of the U2 snRNP particle displaces BBP and its binding partner Mud2p (the homolog of mammalian U2AF65) from the branchpoint region to permit base pairing between the U2 snRNA and the pre-mRNA branchpoint consensus (4). The displacement of BBP and Mud2p from the branchpoint region correlates with a weakening of the U1 snRNP association with the splicing apparatus, an apparent requirement for subsequent binding of U6 snRNA at the 5′ splice site. Although U2 snRNA basepairs with the pre-mRNA substrate, initial U2 snRNP contact is likely protein-mediated and, in mammals, may be accomplished in part through U2AF65 interaction with the SAP155 subunit of the U2 snRNP particle (also called SF3b155) (5). Two-hybrid interaction between Mud2p and the *Saccharomyces cerevisiae* SAP155 homolog, Hsh155p, suggest that this interaction is conserved in yeast, implicating Mud2p function after the U1-snRNP-dependent step of commitment complex formation (6). While U1 displacement appears mediated by Prp28p, stable U2 snRNP addition requires participation of the Prp5p and Sub2 DExD/H-box proteins. Other DExD/H-box proteins promote subsequent steps in spliceosome assembly (Brr2p, Prp2, Prp16p) and product release (Prp22p and Prp43p) (7,8).

U2AF65 is recovered from mammalian cells as a heterodimer with U2AF35, a protein that crosslinks to the 3′ splice site during spliceosome assembly (9–11). Homologs of U2AF35 are broadly represented in nature and have been shown to function in splicing in man, flies, nematodes and fission yeast (11–14). Since no U2AF35 homolog is obvious in budding yeast, Mud2p may have diverged to the degree that it acts independently or simply no longer provides an anchor for 3′ splice site recognition factors. Alternatively, a structurally distinct

*To whom correspondence should be addressed. Tel: 859 257 5530; Fax: 859 257 1717; Email: rymond@uky.edu
Present address:
Qiang Wang, Department of Medicine, Division of Biological Sciences, The University of Chicago, 5841 S. Maryland Ave., Chicago, IL 60637, USA

but functionally related protein may bind Mud2p to serve this purpose or otherwise facilitate co-transcriptional assembly of the yeast mRNP (15).

BBP interacts with at least two essential U1 snRNP proteins, Prp39p and Prp40p, in addition to Mud2p in a step that commits the pre-mRNA to the splicing pathway (3,16). While mammalian U2AF65 binds a critical polypyrimidine stretch upstream of the 3′ splice site and is required for splicing, yeast splicing does not require either a polypyrimidine element or Mud2p (4,17,18). The yeast branchpoint motif is more rigorously conserved than the mammalian sequence, however, and BBP is necessary for yeast cell viability. The loss of either BBP or Mud2p increases pre-mRNA abundance in the cytoplasm (19,20), thereby linking both proteins to the nuclear retention of newly transcribed RNA (21). While BBP and Mud2p bind one another *in vitro*, the degree to which these proteins act in a concerted or independent function during spliceosome assembly or nuclear pre-mRNA retention *in vivo* is less clear.

Here, we report the results of experiments designed to investigate the composition and function of cellular Mud2p and BBP complexes. Like U2AF65, Mud2p is found to exist as a heterodimer. However, rather than interacting with a U2AF35 counterpart, Mud2p, is recovered bound to BBP. The phylogenetically conserved BBP–Mud2p interaction [(22,23) and references within] does not require RNA association and can be isolated essentially free of other splicing factors at modest salt concentration. Evidence is provided to show that four proteins interacting with both BBP and Mud2p in the two-hybrid assay bind one protein of this pair directly and the other through a BBP–Mud2p bridge that requires the first 56 amino acids of BBP. Deletion of this sequence from BBP enhances pre-mRNA export from the nucleus and results in pre-mRNA instability, an effect most notable with RNAs containing branchpoint motif mutations. Surprisingly, rather than enhancing the *bbpΔ56* defect, we find that deletion of *MUD2* increases pre-mRNA recovery in the *bbpΔ56* background. Mutations in either gene suppress a null allele of *SUB2*, supporting the view that the BBP–Mud2p heterodimer is an intracellular target of the Sub2p DExD/H-box ATPase that acts in splicing and mRNA export. Together, these data support the existence of a simple BBP–Mud2p commitment factor bridging multiple contacts in spliceosome assembly and raises the intriguing possibility that Mud2p may enhance the turnover of transcripts with aberrant branchpoint–BBP interaction.

MATERIALS AND METHODS

Yeast strains and assays

Yeast strains BY4742 (*MATα his3Δ1 leu2Δ0 lys2Δ0 ura3Δ0*), BY4741 (*MATA his3Δ1 leu2Δ0 met15Δ0 ura3Δ0*), *mud2::KAN* (*MATα, his3Δ1 leu2Δ0 lys2Δ0 ura3Δ0 mud2::KAN*), *smy2::KAN* (*MATα his3Δ1 leu2Δ0 lys2Δ0 ura3Δ0 smy2::KAN), BBP–TAP* (*MATA his3Δ1 leu2Δ0 met15Δ0 ura3Δ0, MSL5-TAP)* and Mud2-TAP (*MATA his3Δ1 leu2Δ0 met15Δ0 ura3Δ0, MUD2-TAP*) were obtained from Open Biosystems (Huntsville, AL, USA). The *bbpΔ56* mutation was introduced by inverse PCR (5′TAGTGGATCCCTAACTAGGGAACAAATA3′ and 5′TAGGGATCCCATCAACAATTTCCTTTTATTGTG3′) on plasmid pRS414-BBP (obtained from Michael Rosbash). The deletion derivative was then subcloned into YIpLac 211 (24), linearized with BglII and introduced into the genome by two-step replacement into wild-type yeast to generate the *bbpΔ56* strain. FOA selected colonies were scored for excision of the wild-type BBP allele by PCR. The double mutant strains were created using standard yeast genetic techniques (25). The wild-type *MUD2* and *BBP* genes with approximately 300 bp of flanking sequence were subcloned by PCR into YCplac22 (24) for complementation studies. The structures of all novel constructs were confirmed by DNA sequencing prior to use. Plasmids containing the *RPS17A*-based Acc (splicing), Nde/Acc (export) and SD5 (no intron) lacZ reporters genes were previously described in detail (26,27). The lacZ reporter strains were induced with 2% galactose in complete medium at 30°C for 4 h prior to β-galactosidase measurements. Each assay was replicated 4–10 times and pair wise comparisons of the normalized enzyme units were made using a two-tailed *t*-test of significance.

Yeast two hybrid studies were conducted with full-length PCR products (primer sequences available upon request) fused to the *GAL4* DNA binding (DB) and activation domains (AD) on vectors pACT and pAS2, respectively, in yeast strain pJ69-4A (28). The yeast transformants were scored for transactivation of the endogenous reported genes by colony growth at 30°C on medium lacking adenine or on medium lacking histidine and containing 20 mM 3-aminotriazole. Autostimulation of the chromosomal reporter genes was scored in the recombinant pAS2 and pACT transformants in the absence of the binding partner.

RNA analysis

RNA was recovered by breaking yeast on a vortex mixer with sterile glass beads followed by multiple extractions using phenol:chloroform:isolamyl alcohol (25:24:1) and ethanol precipitation. Primer extension was performed on 12–24 μg of total RNA using a ^{32}P end-labeled *RPS17A* exon II primer RB1 (5′CGCTTGACGGTCTTGGTTC3′) and Superscript reverse transcriptase (Invitrogen) at 37°C for 1 h (29). The cDNA products were resolved on a denaturing 7 M urea 5% polyacrylamide gel. Northern blot analysis was performed with the *RPS17A* and *ADE3* hybridization probes on RNA resolved by electrophoresis on a 1% agarose formaldehyde gel and transferred to a charged nylon membrane (30,31). Band intensities were visualized Typhoon 9600 phosphorimager and quantified with Image Quant software GE Healthcare (Piscataway, NJ, USA).

Protein analysis

Conditions for metabolically labeling yeast proteins with Trans ^{35}S-label (ICN) were previously described in detail (32). In short, yeast were labeled for 4 h at

30°C and then broken with glass beads in buffer A [10 mM HEPES (pH 7.9), 10 mM KCl, 200 mM NaCl, 10% glycerol, 0.5 mM dithiothreitol, 0.5 mM phenylmethylsulfonyl fluoride, 2 mM benzamide, 0.5% NP-40] and the lysate cleared by centrifugation at 14 000*g*. Sequential protein A agarose and calmodulin agarose affinity (TAP) selection was done as previously modified (32). Samples recovery was estimated using with Image Quant software GE Healthcare (Piscataway, NJ, USA). Large-scale TAP selection was performed similarly with 10 l of yeast broken under liquid nitrogen in buffer A with a Spex Certiprep 5850 freezer mill (6). The recovered proteins were digested with trypsin, concentrated with a C18 column, and resolved by two-dimensional liquid chromatography followed by mass analysis with a Deca Quadruopole ion trap mass spectrometer (ThermoElectron, Waltham, MA, USA). RNase digestions were performed using RNase A at 20 μg/ml Sigma (St. Louis, MO, USA) or Ambion RNase cocktail (Ambion, Applied Biosystems, Austin TX, USA) at a 1/25 dilution for 30 min at room temperature prior to TAP selection. The mass intensity lists were screened against the non-redundant National Center for Biotechnology Information database using MASCOT software (Matrix Science, Boston, MA, USA) filtered with the default cutoff score of 20. Western blot confirmation of the TAP-selected protein was done using an antibody directed against the residual calmodulin-binding protein (CBP) (anti-CBP; Santa Cruz Biotechnology, Inc. Santa Cruz, CA, USA). The whole TAP epitope was assayed by western blot using a horseradish peroxidase anti-horseradish peroxidase antibody, PAP (Sigma) as described (33).

Size fractionation was performed by resolving 50 μl of calmodulin-agarose selected BBP–TAP or Mud2–TAP complex on a Shimadzu model LC2010C HPLC fitted with the 2 ml injection loop and tandem 15 cm Chromegapore MSE P columns of 2000A and 300A pore diameter. Chromatography was conducted in 200 mM NaCl, 50 mM Tris-HCL, pH 8.0, 0.1% NP40 at 0.5 ml/min. Proteins from alternate fractions were concentrated by TCA precipitation and analyzed by western blot using the anti-horse radish peroxidase antibody (Sigma).

RESULTS

Mud2p and BBP bind one another *in vivo*

To screen for proteins that interact with Mud2p, we metabolically labeled yeast with ^{35}S-amino acids for 4 h and then used tandem affinity purification [TAP (33)] to identify co-purifying factors (Figure 1A, lane 1). In contrast to snRNP or spliceosome preparations previously assayed in this way (32–35), the pattern of ^{35}S-labeled proteins recovered with Mud2-TAP at 200 mM NaCl is quite simple, with the 65 kDa fusion protein derivative, Mud2-CBP, and a single additional band that migrates as a 57 kDa protein. Mud2-CBP consists of the native Mud2 protein joined to ~5 kDa of CBP sequence that persists after TAP (33). Confirmation of the Mud2-CBP assignment was made by western blot using an anti-CBP antibody (see Materials and methods section). A few minor bands are also seen in this preparation, several which appear as background in the untagged control sample (lane 4 and see Figure 3D). RNase A is included at levels sufficient to degrade all detectable full-length rRNA and splicing-relevant snRNA (Figure 1C) although the pattern of recovered proteins appears equivalent without RNase addition (e.g. compare Figure 1A lanes 3 and 6).

In a parallel culture, yeast that express a TAP-tagged BBP derivative were similarly scored for the pattern of recovered proteins. Here also two prominent proteins, 63 and 60 kDa in apparent molecular weight were recovered (Figure 1A, lane 3). Western analysis shows that the 63 kDa band is BBP–CBP, which migrates more slowly than predicted for this 55 kDa fusion protein (data not shown). The 57 kDa and 60 kDa proteins that co-purify with Mud2–TAP and BBP–TAP, respectively, are roughly the predicted sizes for native BBP (50 kDa) and Mud2p (60 kDa). In agreement with this assignment, when Mud2p and BBP are both expressed as TAP-tagged derivatives, the pattern of recovered proteins is equivalent except that the bands corresponding to the untagged BBP and Mud2p are now absent (lane 2).

Although the background is somewhat higher, a similar protein pattern is seen when the isolation is scaled up and unlabeled Mud2–TAP or BBP–TAP complexes are visualized with Coomassie blue (Figure 1B; data not shown). Mass spectrometry was used to confirm the p60-Mud2p assignment and identifies BBP and ribosomal protein Rpl4p in the preparation (see Materials and methods section). While not ruling out the possibility of functional association, we note that the Rpl4p band appears to be of lower abundance than Mud2p or BBP in the preparative (Coomassie blue-stained) sample and that it co-migrates with a background band in the radiolabeled preparations, suggesting that Rp14p may be a contaminant of the preparation. Lower scoring mass analysis signatures were sometimes observed for splicing factors Prp40, Prp8, Prp28, Brr2p, Prp6 and Isy1 as well as for the heat shock protein, Ssb2, and for the Ded1p and Dbp2p DExD/H-box factors. Since none of these proteins correspond to prominent ^{35}S-labeled bands or Coomassie stained proteins, the associations likely reflect weak or transient interactions with the BBP–Mud2p complex or the presence of a small amount of a more elaborate (multisubunit) complex.

The BBP–Mud2p complex is predominantly a heterodimer

The cellular levels of BBP and Mud2p appear equivalent (36) and the Coomassie blue stained BBP and Mud2p bands are of similar intensity, suggesting a 1:1 stoichiometry in the recovered sample. In support of this, after normalization for the greater sulfur content of Mud2p, the 35-S ratio of the metabolically labeled proteins was calculated to be approximately 1.15 when Mud2-TAP is used as bait and 0.87 when BBP–TAP is used as bait. While supportive of equimolar recovery, these experiments do not distinguish between a BBP–Mud2p heterodimer and higher order complexes. To address this, we resolved the calmodulin agarose purified Mud2–BBP

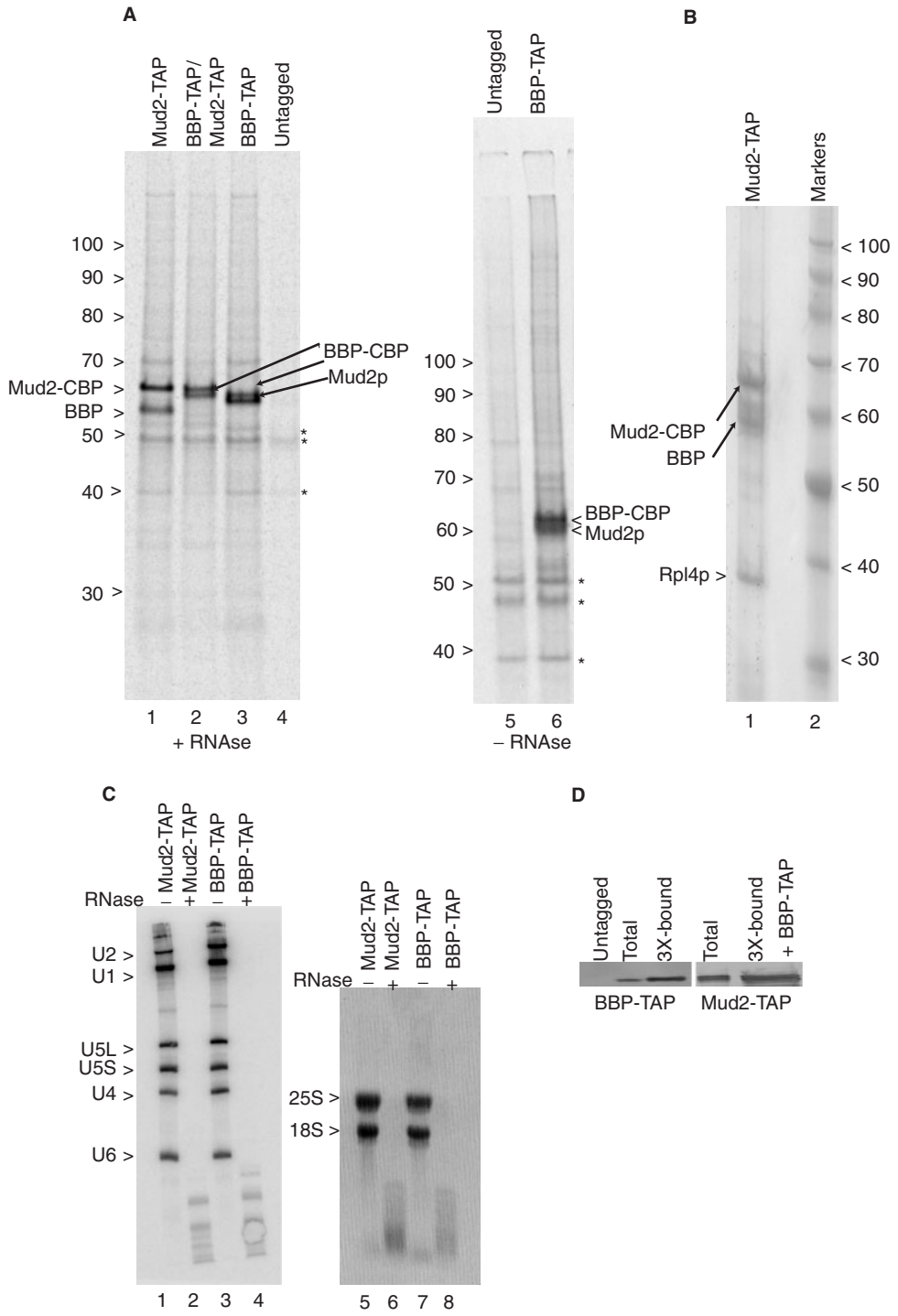

Figure 1. Tandem affinity purification of BBP–TAP and Mud2–TAP. (**A**) Autoradiogram of a 7% polyacrylamide gel of metabolically labeled proteins selected by sequential IgG agarose and calmodulin agarose chromatography from yeast that express the indicated TAP-tagged gene constructs as genomic integrants. The untagged lane shows background proteins (asterisks). Samples in lanes 1–4 were pre-treated with RNase A prior to TAP selection while samples 5–6 were not. The numbers at the left indicate the positions of unlabeled protein molecular weight markers. Bands corresponding to the untagged Mud2p and BBP proteins and the proteins with the residual CBP tags are indicated. (**B**) Coomassie blue stain of unlabeled Mud2-TAP and co-purifying proteins. Lane 2 shows the migration of protein molecular weight markers. (**C**) Yeast used in panel a treated (+) or not (−) with RNase A hybridized with probes specific for the spliceosomal snRNAs (lanes 1–4) or stained with ethidium bromide for the 25S and 18S ribosomal RNAs (lanes 5–8). (**D**) Single-step recovery of BBP–TAP and Mud2–TAP by TAP by calmodulin agarose chromatography. To avoid band distortion due to sample overloading, the unfractionated (total) protein lanes contain 1/3 the equivalent amount of sample. Untagged = calmodulin agarose recovered material recovered from an untagged extract.

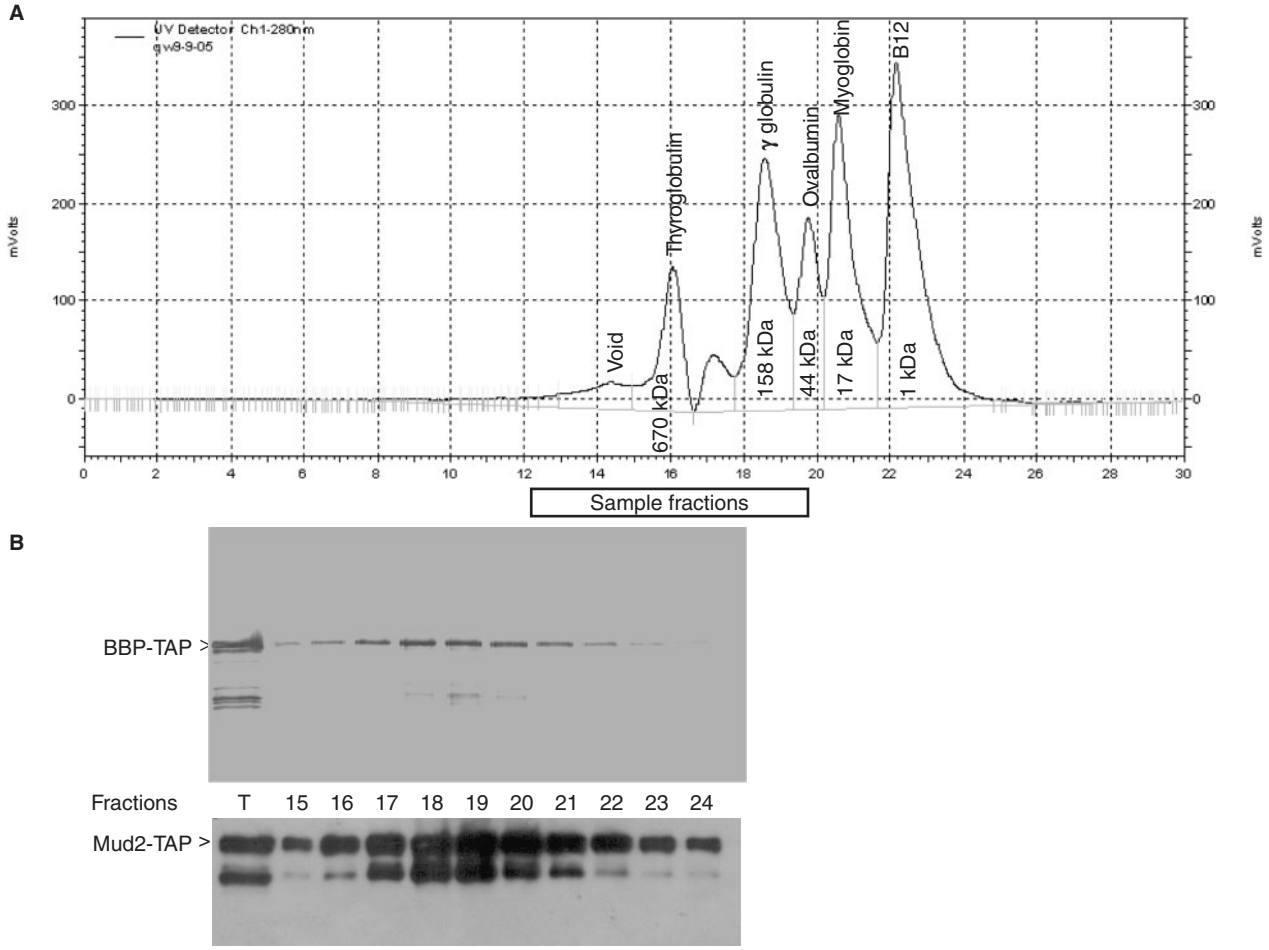

Figure 2. BBP–Mud2p purifies as a heterodimer. (**A**) HPLC resolution of molecular weight standards by sequential 2000Å and 300Å sepharose columns. (**B**) Western blots of the BBP–TAP and Mud2–TAP selected on calmodulin agarose and resolved by HPLC. The blots were developed with an antibody against the TAP epitope. T, total protein applied to the tandem size exclusion columns. The sample numbers correspond to the same column fractions indicated in (A).

complex by tandem HPLC with 2000Å and 300Å sepharose columns. Complex recovery is generally quite efficient, typically 50–75% (Figure 1D). In contrast to the sharp focus of the molecular weight standards (Figure 2A), the BBP–TAP selected complex resolves as a broad peak with the greatest recovery between fractions 18–20 (Figure 2B, upper panel, note that here the protein is visualized with an antibody against the TAP tag, consequently only a single protein is visible). An equivalent distribution is seen when Mud-TAP is used for selection (Figure 2B, lower panel). The highest signals for BBP–TAP and Mud2–TAP correspond to fractions overlapping the γ globulin (158 kDa) and ovalbumin (44 kDa) protein standards. As we previously found no evidence for homodimerization of either Mud2p or BBP (6), this pattern indicates the presence of significant amounts of a BBP–Mud2p heterodimer, which has a predicted mass of ~130 kDa (including the full TAP epitope). Given the spread of signal and the somewhat greater recovery of the TAP tagged partner indicated by the metabolic labeling experiment, monomeric BBP–TAP (73 kDa) and Mud2–TAP (80 kDa) are likely present as well. While the existence of higher order structures (e.g. tetrameric) cannot be ruled out, such complexes are not abundant under these isolation conditions.

Bridging interactions contribute to the previously reported two hybrid interactions of BBP and Mud2p

Four proteins, splicing factors Clf1p, Prp39p and Mer1p, and the largely uncharacterized Smy2 protein have been reported to interact with both BBP and Mud2p by the two-hybrid assay (3,6,37–39). These interactions presumably reflect protein-based contacts made by BBP and Mud2p during spliceosome assembly or in other functional contexts (see Discussion section). Since BBP and Mud2p bind one another we thought it is possible that indirect (i.e. bridging) interactions might contribute to the observed two hybrid pattern. As a first step in addressing this issue, we sought confirmation of the reported interactions using full-length protein constructs. Although differences exist in the extent of host cell reporter gene transactivation, each two-hybrid pair shows detectable activity in the wild-type yeast (Figure 3A). For most constructs, the two hybrid

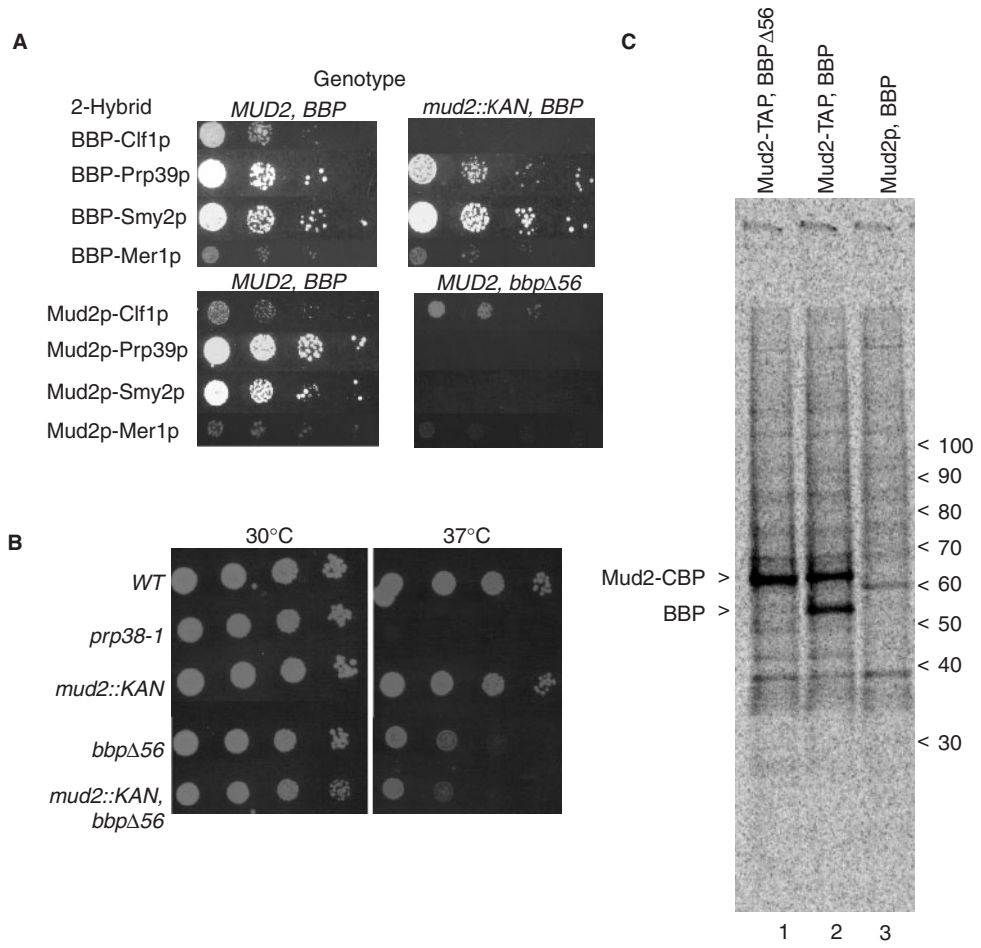

Figure 3. Bridged interactions of the BBP–Mud2p heterodimer. (**A**) Two hybrid interactions conducted in yeast wild-type for both genes (*MUD2, BBP*), deleted for *MUD2* (*mud2::KAN, BBP*), or containing a non-lethal mutation within *BBP* (*MUD2, bbpΔ56*). Reporter gene activity was scored after 3 days at 30°C. (**B**) Direct growth assay in the absence of 2-hybrid plasmids of yeast with wild-type *MUD2* and *BBP* alleles (WT), deleted for *MUD2* (*mud2::KAN, BBP*), containing a non-lethal mutation within BBP (*MUD2, bbpΔ56*) or both mutations (*mud2::KAN, bbpΔ56*) at 23 and 37°C. (**C**) Tandem affinity selection of metabolically labeled proteins with Mud2–TAP from yeast that express the *bbpΔ56* allele (lane 1) and wild-type *BBP* allele (lane 2). Lane 3 shows background proteins isolated from an untagged strain. The positions of unlabeled protein markers are shown on the right.

interactions are reciprocal when the *GAL4* DNA-binding and transactivation domains are swapped. Autostimulation by *CLF1* and *PRP39* in the DNA binding cassette prevented this determination in these two cases.

Since *MUD2* is not essential, the BBP associations can be assayed in the *mud2::KAN* null background to learn which, if any, is Mud2p-dependent. The Prp39p, Mer1p and Smy2p signals all persist in the *mud2::KAN* mutant, showing that none of these proteins require Mud2p for BBP association (Figure 3A). In contrast, the Clf1p-BBP signal is lost in the *mud2::KAN* mutant, strongly suggesting that binding of this essential splicing factor with BBP is indirect and bridged through Mud2p.

The two-hybrid results presented earlier, support direct association of BBP with Prp39p, Mer1p and Smy2p but do not rule out independent interactions of these proteins with Mud2p. As BBP is required for cell viability, we cannot assay for Mud2p-based interactions in its absence. We reasoned, however, that mutation of the Mud2p interaction domain of BBP would not be a lethal and would allow us to score for bridged two-hybrid associations. Previous studies localized the Mud2p binding site to the N-terminal half of BBP [see (19), (40) and references within]. We created a *BBP* derivative, *bbpΔ56*, from which only the most N-terminal region of the proposed interaction domain was deleted and tested this derivative for biological activity. The *bbpΔ56* allele complements the lethality of *bbp::KAN* although the mutant grows more slowly at both 30°C and 37°C than wild-type yeast or the *mud2::KAN* mutant (Figure 3B). While BBP is readily affinity purified with Mud2-TAP, no band unique to the *bbpΔ56* sample can be recovered with Mud2-TAP (Figure 3C compare lane 1 with lanes 2 and 3). Thus, unlike the full length protein, BbpΔ56p does not stably bind Mud2p.

Since BbpΔ56p impairs or blocks Mud2p binding, proteins which interact with Mud2p through a BBP-dependent bridge were anticipated to show reduced or abolished two-hybrid signals in the *bbpΔ56* background. As seen in Figure 3A, Mud2p continues to interact with

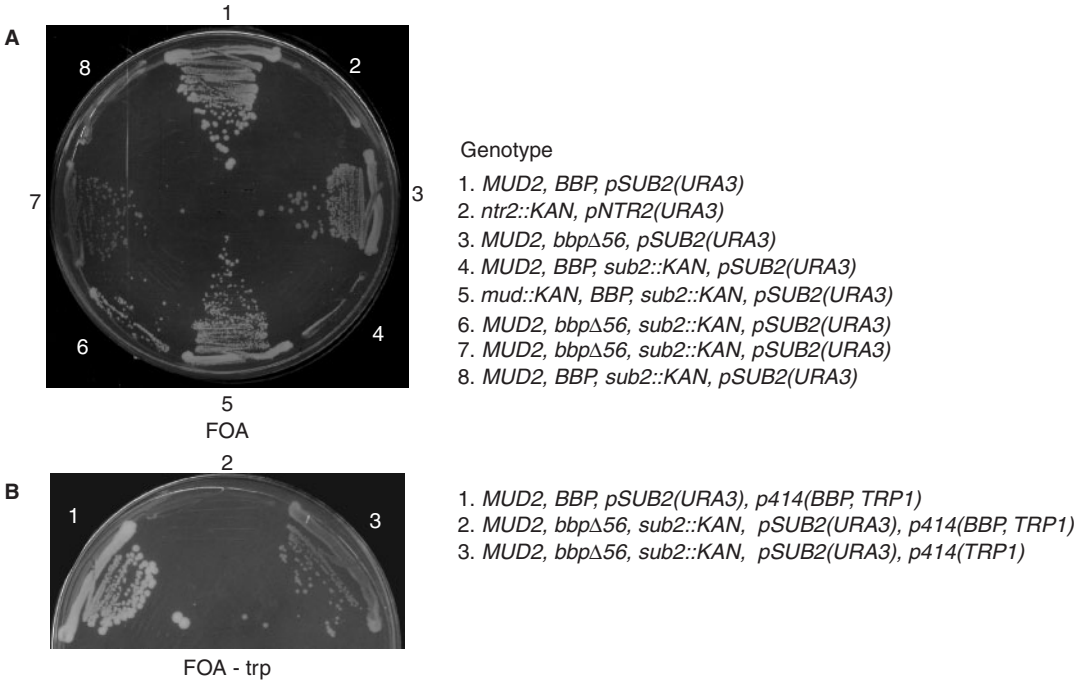

Figure 4. Mutation of the Mud2p interaction domain of BBP suppresses *sub2::KAN* lethality. (**A**) Yeast being the wild-type or the indicated mutant alleles of the *MUD2, BBP, SUB2* transformed with a *URA3*-linked plasmid copy of *SUB2* [*pSUB2*(*URA3*)] plated at 30°C on FOA medium to select for plasmid loss. The fully wild-type strain (steak 1) and a mutant in the essential *NTR2* gene (*ntr2::KAN*) complimented by a *URA3*-linked wild-type plasmid (*pNTR2*(*URA3*)) are included as positive and negative controls for growth, respectively. Streaks 6 and 7 are different meiotic isolates bearing the same *bbpΔ56* mutation. (**B**) Re-introduction of a functional *BBP* allele (or an empty vector, streak 3) on a second plasmid in wild-type yeast (steak 1) or the *bbpΔ56* background (streak 2). Each strain also is transformed with the *pSUB2*(*URA3*) plasmid. Growth is for 3 days at 30°C FOA medium without tryptophan.

Clf1p under these conditions while the Prp39p, Smy2p and Mer1p two-hybrid interactions are lost. Based on this, we propose that Clf1p most likely binds Mud2p directly and that Prp39p, Mer1p and Smy2p interact with Mud2p through a BBP-dependent bridge.

Previously, Guthrie and colleagues (41) showed that deletion of *MUD2* suppresses the lethality (or near lethality) of a *sub2* loss-of-function allele, suggesting that the dissociation of Mud2p from pre-mRNA is an important function of Sub2p. Our results show that Mud2p and BBP bind one another *in vivo*, raising the possibility that the BBP–Mud2p heterodimer is the target of Sub2p activity. To investigate this further we tested whether the *bbpΔ56* mutation likewise compensates for the loss of *SUB2*. Here a *URA3*-marked plasmid copy of *SUB2* [i.e. p*SUB2*(*URA3*)], was introduced into yeast bearing a chromosomal *sub2::KAN* null allele in a wild-type background or in the presence of either the *mud2::KAN* or the *bbpΔ56* mutation (Figure 4A). When selected for plasmid loss on five floroorotic acid (FOA) medium, no visible colonies form after 3 days at 30°C with the *sub2::KAN* mutant in an otherwise wild-type background (streaks 4 and 8) confirming the vital requirement for Sub2p function. Similar results are seen with a control strain in which a lethal *ntr2::KAN* mutation is complemented by a *URA3*-linked plasmid that expresses a functional *NTR2* allele (streak 2). In contrast, the *mud2::KAN, sub2::KAN* double mutant (streak 5) and the *bbpΔ56, sub2::KAN* double mutant (streaks, 6 and 7) are viable in the absence of the p*SUB2*(*URA3*) plasmid. Importantly, re-introduction of a plasmid-based wild-type copy of *BBP* on a *TRP1*-marked plasmid in the *bbpΔ56, sub2::KAN* double mutant background restores the essentiality of p*SUB2*(*URA3*) (i.e. p414-*BBP*, *TRP1*; Figure 4B, streak 2). As expected, this same strain transformed an empty vector (i.e. p414-*TRP*; streak 3) or a wild-type yeast strain transformed with the p414-*BBP*, *TRP1* plasmid (streak 1) continue to form colonies after p*SUB2*(*URA3*) loss. The ability of both *mud2::KAN* and *bbpΔ56* to suppress *sub2*::*KAN* lethality bolsters the view that BBP and Mud2p functionally interact *in vivo* and strongly suggests that the BBP–Mud2p heterodimer is a substrate for Sub2p.

Deletion of *MUD2* suppresses pre-mRNA loss in the *bbpΔ56* background

Since BBP and Mud2p are believed to act cooperatively in branchpoint binding, yeast with the *mud2::KAN* or *bbpΔ56* mutations might be expected to show similar growth characteristics if the only consequence of *bbpΔ56* was the loss of Mud2p interaction. However, the *bbpΔ56* mutant and the *mud2::KAN*, *bbpΔ56* double mutant grow more slowly than the *mud2::KAN* strain, suggesting that some additional function of BBP is impaired by the *bbpΔ56* lesion (Figure 3B). When pre-mRNA is assayed at 23°C, the mRNA to pre-mRNA ratio (a measure of splicing efficiency) of the *RPS17A* transcript appears almost equivalent in the wild-type, single and double

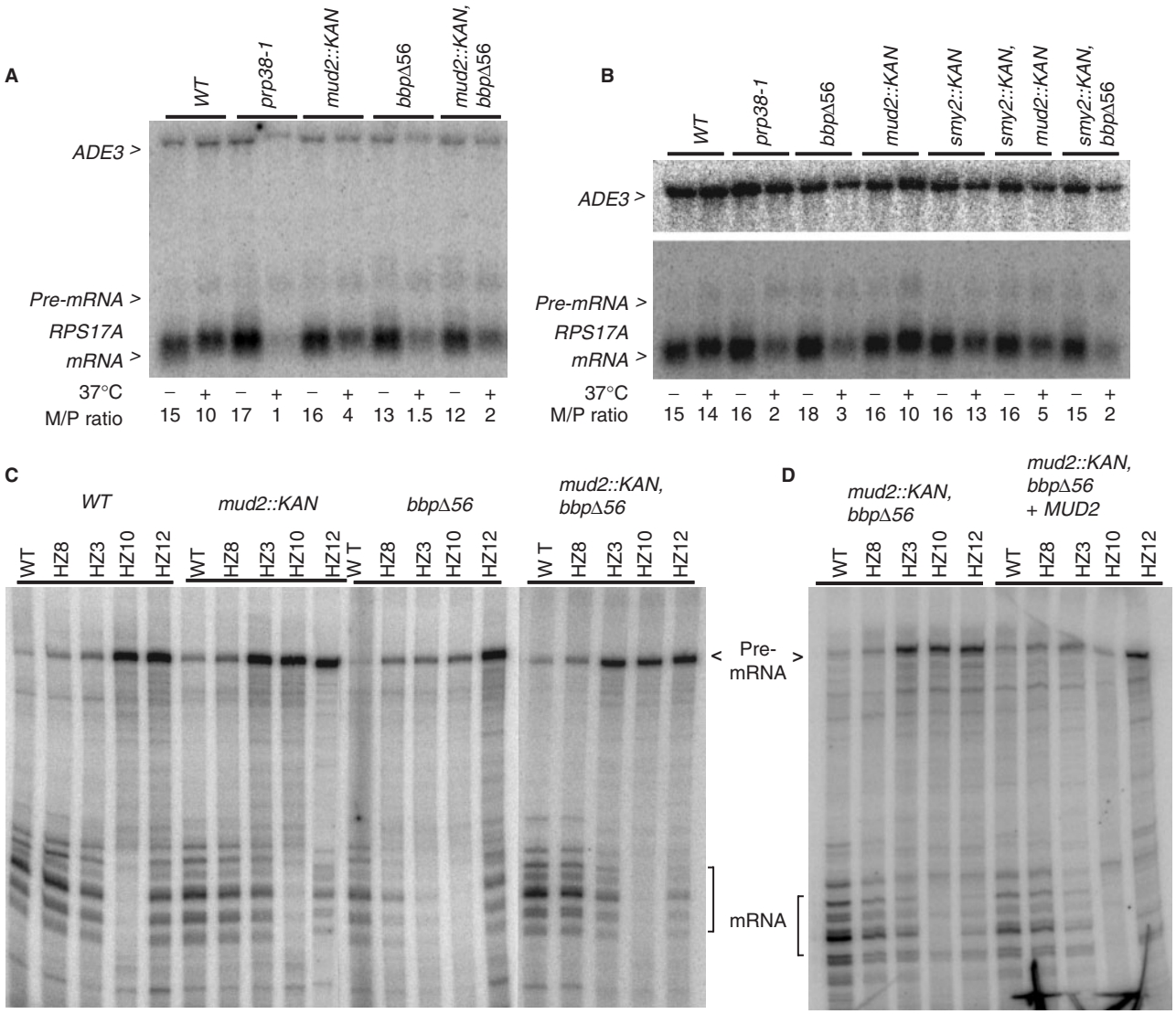

Figure 5. Splicing inhibition by the *mud2::KAN* and *bbΔ56* mutations. (**A**) Northern analysis of RNA extracted from wild-type yeast (WT), the ts splicing mutant, *prp38-1*, and yeast with the *bbpΔ56* and *mud2::KAN single* mutations and with the combined *bbpΔ56* plus *mud2::KAN* double mutant background. RNA harvested from yeast grown continuously at 23°C (−) and after a 2 h shift to 37°C (+) was hybridized with radiolabeled probes to detect the intronless *ADE3* mRNA and the *RPS17A* pre-mRNA and mRNA. The relative abundance of mRNA and pre-mRNA (M/P ratio) is presented below the image. (**B**) Northern analysis as in panel A with added samples *smy2::KAN* and *smy2::KAN* combined with *bbpΔ56* or *mud2::KAN*. (**C**) Primer extension analysis of RNA isolated from the indicated yeast backgrounds that express *RPS17A* reporter gene constructs with the wild-type intron (WT), branchpoint mutants (HZ8, HZ3, HZ10) and 5′ splice site mutant (HZ12). (**D**) Primer extension of RNA from the *bbpΔ56*, *mud2::KAN* double mutant before (left) and after (right) add back of *MUD2*.

mutant backgrounds (Figure 5A; the intronless *ADE3* mRNA is presented as a sample loading control). At 37°C, splicing is more impaired in the *mud2::KAN* mutant when compared to the wild-type strain although it remains better than what is observed after inactivation of the essential U4/U6.U5 tri-snRNP protein, Prp38-1p (30). The *bbpΔ56* mutant has a somewhat stronger splicing defect than that seen with *mud2p::KAN* mutant at 37°C, consistent with the lower vitality of this strain. We see no exacerbation of this splicing defect in the *mud2::KAN*, *bbpΔ56* double mutant background (Figure 5A and see below), however. While there is some experimental variability in splicing efficiency with temperature shift, we see no clear splicing defect with the *smy2::KAN* knockout mutant and no reproducible exacerbation of the *mud2::KAN* or *bbpΔ56* splicing defects by this mutation (Figure 5B).

We next investigated the impact of the *mud2::KAN* and *bbpΔ56* deletions on *RPS17A* reporter gene transcripts with splice site consensus mutations (26). For wild yeast, the pre-mRNA to mRNA ratio increases only modestly when the branchpoint consensus, UACUAAC, is changed to UAUUAAC (HZ8) or UCCUAAC (HZ3) while splicing is essentially abolished when the branchpoint nucleotide is changed in UACUACC (HZ10) [Figure 5C and (26)]. A 5′ splice site mutant, GUAUGU ->GUAUAU (HZ12), also shows a decrease in splicing efficiency in wild-type yeast. In the *mud2::KAN*

background, these splicing defects are modestly exacerbated with the greatest impact seen with HZ3 where the pre-mRNA/mRNA ratio increases ~2-fold compared to the wild-type strain.

Reporter transcript splicing in the *bbpΔ56* background showed two distinctive features. First, although this lesion is outside the RNA binding KH domain core (approximately amino acids 149–133), splicing is much more sensitive to mutations at the branchpoint consensus when compared with wild-type yeast or the *mud2::KAN* mutant; splicing of the 5′ splice site mutant appears largely unaffected. Second, even as mRNA levels drop, pre-mRNA levels do not accumulate to the degree observed with wild-type or *mud2::KAN* yeast. This characteristic is especially obvious with the HZ3 and HZ10 substrate mutations and is consistent with the observation that diminished BBP activity results in leakage of unprocessed pre-mRNA into the cytoplasm where it is sensitive to turnover by nonsense-mediated decay (42). Surprisingly, the pre-mRNA accumulation defect of *bbpΔ56* is largely suppressed in the *bbpΔ56, mud2::KAN* double mutant background. This is most easily seen with the HZ3 substrate where pre-mRNA levels are 2- to 3-fold higher than with *bbpΔ56* alone. Although a more subtle change; spliced mRNA also appears to increase (here by ~35% when normalized to background bands) in the *bbpΔ56, mud2::KAN* double mutant. Importantly, transformation with a *MUD2*-containing plasmid reverses this effect, resulting in lowered pre-mRNA levels mostly clearly seen with the HZ3 and HZ10 branchpoint motif mutants (Figure 5D).

Since pre-mRNA is degraded by nonsense-mediated decay in the cytoplasm (42), a reduction in nuclear export of pre-mRNA in the *bbpΔ56, mud2::KAN* background might contribute to the increased pre-mRNA recovery. To learn if this is the case, we used two previously described splice-sensitive reporters in which the lacZ gene is inserted into exon 2 in frame with either the upstream exon (to monitor splicing) or with the intron (to monitor translation of pre-mRNA exported from the nucleus) (27). Unlike the reporter genes described before (Figure 5), the intron of this export reporter contains no pre-mature translational termination codons and remains stable in the cytoplasm (27). To better control genetic variability, β-galactosidase measurements were made in the *bbpΔ56, mud2::KAN* double mutant before and after reintroduction of either *MUD2* or *BBP* (see Materials and methods section). The β-galactosidase values are adjusted for variation in gene induction by normalization with an intronless reporter cassette (19,20).

Consistent with the earlier studies (19,20), deletion of *MUD2* enhances nuclear pre-mRNA export about 2-fold and results in reduced expression from the inherently inefficiently spliced mRNA reporter (Figure 6). The *bbpΔ56* mutant shows a greater reduction in spliced mRNA expression and a corresponding increase in signal from the unprocessed pre-mRNA. Rather than decreasing, β-galactosidase levels increase with export reporter in the *bbpΔ56, mud2::KAN* double mutant background compared to either single mutant. Based on this, we conclude that the increase in pre-mRNA abundance noted

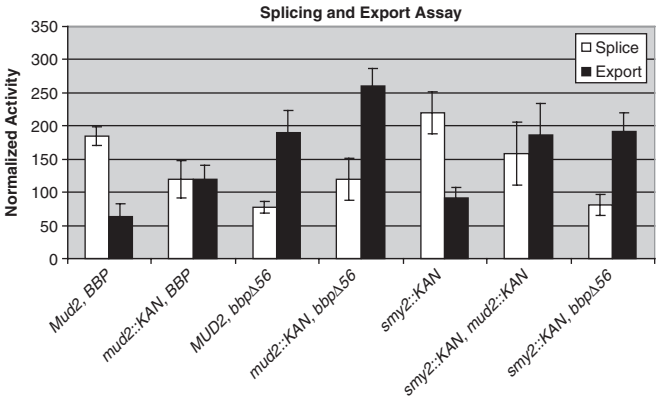

Figure 6. Increased RNA export reporter activity in the *mud2::KAN*, *bbΔ56* and *mud2::KAN*, *smy2::KAN* double mutant backgrounds. β-galactosidase activities from the spliced reporter and unspliced reporters are presented in the wild-type and mutant backgrounds. The β-galactosidase measurements were normalized by dividing each by that obtained with an intronless control reporter assayed in parallel and multiplying the resultant value by 1000. The bars represent the experimental standard deviations from four to ten replicate experiments. A two-tailed *t*-test of significance was used with pair wise comparisons.

before for the *bbpΔ56, mud2::KAN* double mutant (Figure 5C and D) cannot be due to a simple reduction in the amount of pre-mRNA exported to the cytoplasm. We note that the signal from the inefficiently spliced reporter also appears to increase slightly in the *bbpΔ56, mud2::KAN* double mutant when compared with the *bbpΔ56* alone ($P = 0.0008$). While other models are conceivable, these results are consistent with the deletion of *MUD2* increasing the synthesis or stability of pre-mRNA in the *bbpΔ56* background (see Discussion section). Finally, while normal levels of splicing and export are seen with the *smy2::KAN* mutant or with the *smy2::KAN, bbp Δ56* double mutant, when *smy2::KAN* is combined with *mud2::KAN* expression from the export reporter increases significantly ($P = 0.0004$). This genetic interaction suggests a common intracellular function of Smy2p and Mud2p.

DISCUSSION

Specific interactions between BBP and the branchpoint motif occur early in spliceosome assembly that together with the U1 snRNP particle bound to the 5′ splice site contribute to the formation of a nuclear retained structure called the commitment complex (43). *In vitro*, Mud2p binds BBP to enhance substrate association (23) and recent chromatin immunoprecipitation studies suggest an early-acting role for this protein during spliceosome assembly *in vivo* (44). In the mammalian system U2AF65 binds tightly to a smaller U2AF subunit, U2AF35 (45), which, together with DEK(46) and PUF60 (47,48) act in 3′ splice site selection. The *Schizosaccharomyces pombe* (fission yeast) Mud2/U2AF65 homolog also binds a smaller U2AF subunit, U2AF23, as well as stably interacting with the BBP (22). In contrast to the mammalian and fission yeast systems, our studies identify

a BBP–Mud2p heterodimer as the prominent form of these commitment complex proteins in budding yeast and rule out stable association of a U2AF35-like third factor.

Previous two-hybrid and protein-interaction studies localized the Mud2p binding domain between residues 41–141 of BBP (37,40). We have refined the map of critical residues by showing that deletion of BBP residues 2–55 significantly weakens or prevents Mud2p association. The BBP–Mud2p heterodimer bridges at least four common two-hybrid interactions. Of these, the BBP-binding partners Prp39p and Mer1p have established roles in early spliceosome assembly consistent with functional associations with the BBP–Mud2p heterodimer. Prp39p is an essential U1 snRNP protein and extracts where Prp39p is inactive or absent fail to form commitment complexes (49). As such, in addition to BBP-Prp40p (3), BBP-Prp39p bolsters the cross-intron association of U1 snRNP with the 5′ splice site and branchpoint region of the pre-mRNA. Mer1p is a meiosis-specific splicing factor that interacts with the Nam8 and Bud13 proteins to promote early spliceosome assembly [(39,50,51) and references within]. The BBP–Mer1p interaction may help integrate predicted U1 snRNP-Nam8p contacts near the 5′ splice site with the U2 snRNP-Bud13p interactions at the branchpoint on inherently weak splicing substrates (6,52). Although Mud2p is not essential for cell viability, Mud2p binds the U2 snRNP SF3b subunit, Hsh155p, in addition to other U2 snRNP proteins (6,18,37) providing a possible means by which Mud2p may enhance the kinetics of spliceosome assembly (4). The Mud2p two-hybrid partner, Clf1p, also interacts genetically or biochemically with several SF3b or SF3b-associated U2 snRNP proteins [i.e. Hsh155, Rds3, Rse3p, Bud13p; see (6,53)]. And while generally thought to function with the Prp19 complex (NTC) late in splicing (54), an earlier role for Clf1p in spliceosome assembly has been suggested (32,55). Indeed, a solution structure was recently presented for the N-terminus of Clf1p interacting with the FF domain of the BBP-binding protein and U1 snRNP component, Prp40p (56). Consequently, Clf1p may act with the BBP–Mud2p complex defined here to influence U1 and U2 snRNP dynamics with the nascent pre-mRNP.

The biological relevance of the Smy2p-BBP interaction to splicing is less clear. *SMY2* was originally identified as a dosage suppressor of a mutation in *MYO2*, a gene encoding the heavy chain of the yeast type V myosin (57). Smy2p contains a GYF motif (58) (amino acids 205–261), a domain that binds proline-rich sequences and that can be found in other splicing factors, including the U5 snRNP-associated CD2BP2 protein (59,60) and yeast Lin 1 (61,62). Although Smy2p is predicted to interact with the proline-rich domains of BBP and Prp8p (63), we detect no reduction in splicing efficiency in the *smy2::KAN* mutant or evidence for *smy2::KAN* exacerbating the *mud2::KAN* or *bbpΔ56* splicing defects. We note, however, that Smy2p is also predicted to bind a number of cytoplasmic mRNA decay factors including Eap1p, Pat1p, Kem1p, Mot2p, Ccr4p, Pop2p (64) and that it localizes to cytoplasmic P-bodies enriched in these factors (64). While requiring additional study, the increased RNA export reporter signal in the *mud2::KAN, smy2::KAN* double mutant might reflect stabilization of cytoplasmic pre-mRNA in the absence of Smy2p and Mud2p. Pre-mRNA stabilization was not obvious for natural transcripts in this background (Figure 5) although this might be explained by the normally rapid degradation of pre-RNAs with premature translational termination codons.

The hypersensitivity to branchpoint mutations observed for BbpΔ56p has been with other *BBP* mutations (19) and for each mutant assayed impaired splicing is correlated with enhanced pre-mRNA export from the nucleus. Increased nuclear export of pre-mRNA is not limited to mutants of BBP and Mud2p, however, as mutations in a number of early acting splicing factors and other nuclear proteins also show this defect (37,65–67), indicating considerable complexity to the nuclear retained mRNP. We observe that reduced pre-mRNA recovery with branchpoint motif mutants in the *bbpΔ56* background can be partially suppressed by deletion of *MUD2*, apparently without reducing pre-mRNA export. All else being equal, stabilizing nuclear pre-mRNA in the *mud2::KAN, bbpΔ56* background might be expected to provide increased opportunity both for the precursor to be spliced or exported, both possibilities consistent with the results of our reporter gene assays (Figures 5 and 6). Nuclear pre-mRNA is subject to surveillance by the exosome (68).While the details of exosome target selection are not well understood (69), it seems reasonable that pre-mRNA assembled into spliceosomes will be less sensitive to turnover. The suppression of *sub2::KAN* lethality by *bbpΔ56* and *mud::KAN* argues for the bypass of the Sub2p-dependent step, possibly enhancing spliceosome assembly. A second but not mutually exclusive possibility for the enhanced pre-mRNA recovery in the *mud2::KAN, bbpΔ56* double mutant is that the presence of Mud2p may normally enhance the turnover of intron-bearing pre-mRNA in the cytoplasm. As mutations in the pre-mRNA branchpoint motif increase the level of cytoplasmic pre-mRNA (27), suppression by *mud2::KAN* might reasonably be most pronounced with branchpoint mutants in the *bbpΔ56* background. A cytoplasmic function for Mud2p would be consistent with its localization in both the nucleus and cytoplasm (70), the association of the BBP–Mud2p heterodimer with the P-body linked Smy2p, and with the observation that the metazoan U2AF can be recovered bound to spliced mRNA and to the transcripts of intronless genes (71,72). Finally, given the functional coupling of transcription, splicing, mRNA export, translation and decay [see (73,74) and references within], it is conceivable that Mud2p acts elsewhere in the gene expression pathway to alter cellular pre-mRNA levels.

ACKNOWLEDGEMENTS

We thank Kate Zaytseva and Mingxia Zhang for technical assistance and Charles Query, Stefan Stamm and members of the Rymond lab for their helpful comments on this article. The pRS414-BBP, Acc, Nde/Acc, and SD5 plasmids were generously provided by Michael Rosbash. This work was supported by National Institutes of Health award GM42476 to BCR and infrastructure support in

proteomics from the National Science Foundation award EPS-0132295. Funding to pay the Open Access publication charges for this article was provided by National Institutes of Health award GM42476 to BCR.

Conflict of interest statement. None declared.

REFERENCES

1. Burge,C.B., Tuschl,T. and Sharp,P.A. (1999) Splicing of Precursors to mRNAs by the Spliceosome. In Gesteland,R.F., Cech,T.R. and Atkins,J.F. (eds). *The RNA World*, 2nd edn. Cold Spring Harbor Laboratory Press, Cold Spring Harbor, NY.
2. Kramer,A. and Utans,U. (1991) Three protein factors (SF1, SF3 and U2AF) function in pre-splicing complex formation in addition to snRNPs. *EMBO J.*, **10**, 1503–1509.
3. Abovich,N. and Rosbash,M. (1997) Cross-intron bridging interactions in the yeast commitment complex are conserved in mammals. *Cell*, **89**, 403–412.
4. Rutz,B. and Seraphin,B. (1999) Transient interaction of BBP/ScSF1 and Mud2 with the splicing machinery affects the kinetics of spliceosome assembly. *RNA*, **5**, 819–831.
5. Gozani,O., Potashkin,J. and Reed,R. (1998) A potential role for U2AF-SAP 155 interactions in recruiting U2 snRNP to the branch site. *Mol. Cell Biol.*, **18**, 4752–4760.
6. Wang,Q., He,J., Lynn,B. and Rymond,B.C. (2005) Interactions of the yeast SF3b splicing factor. *Mol. Cell Biol.*, **25**, 10745–10754.
7. Brow,D.A. (2002) Allosteric cascade of spliceosome activation. *Annu. Rev. Genet.*, **36**, 333–360.
8. Staley,J.P. and Guthrie,C. (1998) Mechanical devices of the spliceosome: motors, clocks, springs, and things. *Cell*, **92**, 315–326.
9. Wu,S., Romfo,C.M., Nilsen,T.W. and Green,M.R. (1999) Functional recognition of the 3′ splice site AG by the splicing factor U2AF35. *Nature*, **402**, 832–835.
10. Zorio,D.A. and Blumenthal,T. (1999) Both subunits of U2AF recognize the 3′ splice site in Caenorhabditis elegans. *Nature*, **402**, 835–838.
11. Merendino,L., Guth,S., Bilbao,D., Martinez,C. and Valcarcel,J. (1999) Inhibition of msl-2 splicing by Sex-lethal reveals interaction between U2AF35 and the 3′ splice site AG. *Nature*, **402**, 838–841.
12. Zuo,P. and Maniatis,T. (1996) The splicing factor U2AF35 mediates critical protein-protein interactions in constitutive and enhancer-dependent splicing. *Genes Dev.*, **10**, 1356–1368.
13. Webb,C.J., Lakhe-Reddy,S., Romfo,C.M. and Wise,J.A. (2005) Analysis of mutant phenotypes and splicing defects demonstrates functional collaboration between the large and small subunits of the essential splicing factor U2AF in vivo. *Mol. Biol. Cell*, **16**, 584–596.
14. Zorio,D.A. and Blumenthal,T. (1999) U2AF35 is encoded by an essential gene clustered in an operon with RRM/cyclophilin in Caenorhabditis elegans. *RNA*, **5**, 487–494.
15. Lacadie,S.A., Tardiff,D.F., Kadener,S. and Rosbash,M. (2006) In vivo commitment to yeast cotranscriptional splicing is sensitive to transcription elongation mutants. *Genes Dev.*, **20**, 2055–2066.
16. Berglund,J.A., Chua,K., Abovich,N., Reed,R. and Rosbash,M. (1997) The splicing factor BBP interacts specifically with the pre-mRNA branchpoint sequence UACUAAC. *Cell*, **89**, 781–787.
17. Rymond,B.C. and Rosbash,M. (1985) Cleavage of 5′ splice site and lariat formation are independent of 3′ splice site in yeast mRNA splicing. *Nature*, **317**, 735–737.
18. Abovich,N., Liao,X.C. and Rosbash,M. (1994) The yeast MUD2 protein: an interaction with PRP11 defines a bridge between commitment complexes and U2 snRNP addition. *Genes Dev.*, **8**, 843–854.
19. Rutz,B. and Seraphin,B. (2000) A dual role for BBP/ScSF1 in nuclear pre-mRNA retention and splicing. *EMBO J.*, **19**, 1873–1886.
20. Rain,J.C. and Legrain,P. (1997) In vivo commitment to splicing in yeast involves the nucleotide upstream from the branch site conserved sequence and the Mud2 protein. *EMBO J.*, **16**, 1759–1771.
21. Jensen,T.H., Dower,K., Libri,D. and Rosbash,M. (2003) Early formation of mRNP. License for export or quality control? *Mol. Cell*, **11**, 1129–1138.
22. Huang,T., Vilardell,J. and Query,C.C. (2002) Pre-spliceosome formation in S.pombe requires a stable complex of SF1-U2AF(59)-U2AF(23). *EMBO J.*, **21**, 5516–5526.
23. Berglund,J.A., Abovich,N. and Rosbash,M. (1998) A cooperative interaction between U2AF65 and mBBP/SF1 facilitates branchpoint region recognition. *Genes Dev.*, **12**, 858–867.
24. Gietz,R.D. and Sugino,A. (1988) New yeast-Escherichia coli shuttle vectors constructed with in vitro mutagenized yeast genes lacking six-base pair restriction sites. *Gene*, **74**, 527–534.
25. Kaiser,C., Michaelis,S. and Mitchell,A. (eds) (1994) *Methods in Yeast Genetics*. Cold Spring Harbor Laboratory Press, Cold Spring Harbor, NY.
26. Jacquier,A., Rodriguez,J.R. and Rosbash,M. (1985) A quantitative analysis of the effects of 5′ junction and TACTAAC box mutants and mutant combinations on yeast mRNA splicing. *Cell*, **43**, 423–430.
27. Legrain,P. and Rosbash,M. (1989) Some cis- and trans-acting mutants for splicing target pre-mRNA to the cytoplasm. *Cell*, **57**, 573–583.
28. James,P., Halladay,J. and Craig,E.A. (1996) Genomic libraries and a host strain designed for highly efficient two-hybrid selection in yeast. *Genetics*, **144**, 1425–1436.
29. Teem,J.L. and Rosbash,M. (1983) Expression of a beta-galactosidase gene containing the ribosomal protein 51 intron is sensitive to the rna2 mutation of yeast. *Proc. Natl Acad. Sci. USA*, **80**, 4403–4407.
30. Blanton,S., Srinivasan,A. and Rymond,B.C. (1992) PRP38 encodes a yeast protein required for pre-mRNA splicing and maintenance of stable U6 small nuclear RNA levels. *Mol. Cell Biol.*, **12**, 3939–3947.
31. Pikielny,C.W. and Rosbash,M. (1985) mRNA splicing efficiency in yeast and the contribution of nonconserved sequences. *Cell*, **41**, 119–126.
32. Wang,Q., Hobbs,K., Lynn,B. and Rymond,B.C. (2003) The Clf1p splicing factor promotes spliceosome assembly through N-terminal tetratricopeptide repeat contacts. *J. Biol. Chem.*, **278**, 7875–7883.
33. Puig,O., Caspary,F., Rigaut,G., Rutz,B., Bouveret,E., Bragado-Nilsson,E., Wilm,M. and Seraphin,B. (2001) The tandem affinity purification (TAP) method: a general procedure of protein complex purification. *Methods*, **24**, 218–229.
34. Wang,Q. and Rymond,B.C. (2003) Rds3p is required for stable U2 snRNP recruitment to the splicing apparatus. *Mol. Cell. Biol.*, **23**, 7339–7349.
35. Chen,N., Harris,T.W., Antoshechkin,I., Bastiani,C., Bieri,T., Blasiar,D., Bradnam,K., Canaran,P., Chan,J., Chen,C.K. *et al.* (2005) WormBase: a comprehensive data resource for Caenorhabditis biology and genomics. *Nucleic Acids Res.*, **33**, D383–389.
36. Ghaemmaghami,S., Huh,W.K., Bower,K., Howson,R.W., Belle,A., Dephoure,N., O'Shea,E.K. and Weissman,J.S. (2003) Global analysis of protein expression in yeast. *Nature*, **425**, 737–741.
37. Fromont-Racine,M., Rain,J.C. and Legrain,P. (1997) Toward a functional analysis of the yeast genome through exhaustive two-hybrid screens [see comments]. *Nat. Genet.*, **16**, 277–282.
38. Chung,S., McLean,M.R. and Rymond,B.C. (1999) Yeast ortholog of the Drosophila crooked neck protein promotes spliceosome assembly through stable U4/U6.U5 snRNP addition. *RNA*, **5**, 1042–1054.
39. Spingola,M., Armisen,J. and Ares,M. Jr. (2004) Mer1p is a modular splicing factor whose function depends on the conserved U2 snRNP protein Snu17p. *Nucleic Acids Res.*, **32**, 1242–1250.
40. Rain,J.C., Rafi,Z., Rhani,Z., Legrain,P. and Kramer,A. (1998) Conservation of functional domains involved in RNA binding and protein-protein interactions in human and Saccharomyces cerevisiae pre-mRNA splicing factor SF1. *RNA*, **4**, 551–565.
41. Kistler,A.L. and Guthrie,C. (2001) Deletion of MUD2, the yeast homolog of U2AF65, can bypass the requirement for sub2, an essential spliceosomal ATPase. *Genes Dev.*, **15**, 42–49.
42. He,F., Peltz,S.W., Donahue,J.L., Rosbash,M. and Jacobson,A. (1993) Stabilization and ribosome association of unspliced pre-mRNAs in a yeast upf1-mutant. *Proc. Natl Acad. Sci. USA*, **90**, 7034–7038.

43. Seraphin,B. and Rosbash,M. (1989) Identification of functional U1 snRNA-pre-mRNA complexes committed to spliceosome assembly and splicing. *Cell*, **59**, 349–358.
44. Lacadie,S.A. and Rosbash,M. (2005) Cotranscriptional spliceosome assembly dynamics and the role of U1 snRNA:5′ss base pairing in yeast. *Mol. Cell*, **19**, 65–75.
45. Zamore,P.D. and Green,M.R. (1989) Identification, purification, and biochemical characterization of U2 small nuclear ribonucleoprotein auxiliary factor. *Proc. Natl Acad. Sci. USA*, **86**, 9243–9247.
46. Soares,L.M., Zanier,K., Mackereth,C., Sattler,M. and Valcarcel,J. (2006) Intron removal requires proofreading of U2AF/3′ splice site recognition by DEK. *Science*, **312**, 1961–1965.
47. Hastings,M.L., Allemand,E., Duelli,D.M., Myers,M.P. and Krainer,A.R. (2007) Control of pre-mRNA splicing by the general splicing factors PUF60 and U2AF65. *PLoS ONE*, **2**, e538.
48. Page-McCaw,P.S., Amonlirdviman,K. and Sharp,P.A. (1999) PUF60: a novel U2AF65-related splicing activity. *RNA*, **5**, 1548–1560.
49. Lockhart,S.R. and Rymond,B.C. (1994) Commitment of yeast pre-mRNA to the splicing pathway requires a novel U1 small nuclear ribonucleoprotein polypeptide, Prp39p. *Mol. Cell Biol.*, **14**, 3623–3633.
50. Scherrer,F.W. Jr. and Spingola,M. (2006) A subset of Mer1p-dependent introns requires Bud13p for splicing activation and nuclear retention. *RNA*, **12**, 1361–1372.
51. Engebrecht,J.A., Voelkel-Meiman,K. and Roeder,G.S. (1991) Meiosis-specific RNA splicing in yeast. *Cell*, **66**, 1257–1268.
52. Puig,O., Gottschalk,A., Fabrizio,P. and Seraphin,B. (1999) Interaction of the U1 snRNP with nonconserved intronic sequences affects 5′ splice site selection. *Genes Dev.*, **13**, 569–580.
53. Vincent,K., Wang,Q., Jay,S., Hobbs,K. and Rymond,B.C. (2003) Genetic interactions with CLF1 identify additional pre-mRNA splicing factors and a link between activators of yeast vesicular transport and splicing. *Genetics*, **164**, 895–907.
54. Chen,C.H., Yu,W.C., Tsao,T.Y., Wang,L.Y., Chen,H.R., Lin,J.Y., Tsai,W.Y. and Cheng,S.C. (2002) Functional and physical interactions between components of the Prp19p-associated complex. *Nucleic Acids Res.*, **30**, 1029–1037.
55. Chung,S., Zhou,Z., Huddleston,K.A., Harrison,D.A., Reed,R., Coleman,T.A. and Rymond,B.C. (2002) Crooked neck is a component of the human spliceosome and implicated in the splicing process. *Biophys. Biochem. Acta*, **1576**, 289–297.
56. Gasch,A., Wiesner,S., Martin-Malpartida,P., Ramirez-Espain,X., Ruiz,L. and Macias,M.J. (2006) The structure of Prp40 FF1 domain and its interaction with the crn-TPR1 motif of Clf1 gives a new insight into the binding mode of FF domains. *J. Biol. Chem.*, **281**, 356–364.
57. Lillie,S.H. and Brown,S.S. (1994) Immunofluorescence localization of the unconventional myosin, Myo2p, and the putative kinesin-related protein, Smy1p, to the same regions of polarized growth in Saccharomyces cerevisiae. *J. Cell. Biol.*, **125**, 825–842.
58. Nishizawa,K., Freund,C., Li,J., Wagner,G. and Reinherz,E.L. (1998) Identification of a proline-binding motif regulating CD2-triggered T lymphocyte activation. *Proc. Natl Acad. Sci. USA*, **95**, 14897–14902.
59. Kofler,M., Heuer,K., Zech,T. and Freund,C. (2004) Recognition sequences for the GYF domain reveal a possible spliceosomal function of CD2BP2. *J. Biol. Chem.*, **279**, 28292–28297.
60. Laggerbauer,B., Liu,S., Makarov,E., Vornlocher,H.P., Makarova,O., Ingelfinger,D., Achsel,T. and Luhrmann,R. (2005) The human U5 snRNP 52K protein (CD2BP2) interacts with U5-102K (hPrp6), a U4/U6.U5 tri-snRNP bridging protein, but dissociates upon tri-snRNP formation. *RNA*, **11**, 598–608.
61. Bialkowska,A. and Kurlandzka,A. (2002) Proteins interacting with Lin 1p, a putative link between chromosome segregation, mRNA splicing and DNA replication in Saccharomyces cerevisiae. *Yeast*, **19**, 1323–1333.
62. Stevens,S.W., Barta,I., Ge,H.Y., Moore,R.E., Young,M.K., Lee,T.D. and Abelson,J. (2001) Biochemical and genetic analyses of the U5, U6, and U4/U6 x U5 small nuclear ribonucleoproteins from Saccharomyces cerevisiae. *RNA*, **7**, 1543–1553.
63. Kofler,M.M. and Freund,C. (2006) The GYF domain. *FEBS J.*, **273**, 245–256.
64. Georgiev,A., Sjostrom,M. and Wieslander,A. (2007) Binding specificities of the GYF domains from two Saccharomyces cerevisiae Paralogs. *Protein Eng. Des. Sel.*, **20**, 443–452.
65. Dziembowski,A., Ventura,A.P., Rutz,B., Caspary,F., Faux,C., Halgand,F., Laprevote,O. and Seraphin,B. (2004) Proteomic analysis identifies a new complex required for nuclear pre-mRNA retention and splicing. *EMBO J.*, **23**, 4847–4856.
66. Abovich,N., Legrain,P. and Rosbash,M. (1990) The yeast PRP6 gene encodes a U4/U6 small nuclear ribonucleoprotein particle (snRNP) protein, and the PRP9 gene encodes a protein required for U2 snRNP binding. *Mol. Cell Biol.*, **10**, 6417–6425.
67. Galy,V., Gadal,O., Fromont-Racine,M., Romano,A., Jacquier,A. and Nehrbass,U. (2004) Nuclear retention of unspliced mRNAs in yeast is mediated by perinuclear Mlp1. *Cell*, **116**, 63–73.
68. Houseley,J., LaCava,J. and Tollervey,D. (2006) RNA-quality control by the exosome. *Nat. Rev. Mol. Cell Biol.*, **7**, 529–539.
69. Rougemaille,M., Gudipati,R.K., Olesen,J.R., Thomsen,R., Seraphin,B., Libri,D. and Jensen,T.H. (2007) Dissecting mechanisms of nuclear mRNA surveillance in THO/sub2 complex mutants. *EMBO J*, **26**, 2317–2326.
70. Huh,W.K., Falvo,J.V., Gerke,L.C., Carroll,A.S., Howson,R.W., Weissman,J.S. and O'Shea,E.K. (2003) Global analysis of protein localization in budding yeast. *Nature*, **425**, 686–691.
71. Blanchette,M., Labourier,E., Green,R.E., Brenner,S.E. and Rio,D.C. (2004) Genome-wide analysis reveals an unexpected function for the Drosophila splicing factor U2AF50 in the nuclear export of intronless mRNAs. *Mol. Cell*, **14**, 775–786.
72. Gama-Carvalho,M., Barbosa-Morais,N.L., Brodsky,A.S., Silver,P.A. and Carmo-Fonseca,M. (2006) Genome-wide identification of functionally distinct subsets of cellular mRNAs associated with two nucleocytoplasmic-shuttling mammalian splicing factors. *Genome Biol.*, **7**, R113.
73. Das,R., Yu,J., Zhang,Z., Gygi,M.P., Krainer,A.R., Gygi,S.P. and Reed,R. (2007) SR proteins function in coupling RNAP II transcription to pre-mRNA splicing. *Mol. Cell*, **26**, 867–881.
74. Keene,J.D. (2007) RNA regulons: coordination of post-transcriptional events. *Nat. Rev. Genet.*, **8**, 533–543.